Do folate-receptor targeted liposomal photosensitizers enhance photodynamic therapy selectivity?

María García-Díaz[a], Santi Nonell[a], Ángeles Villanueva[b], Juan C. Stockert[b], Magdalena Cañete[b], Ana Casadó[c], Margarita Mora[c], M. Lluïsa Sagristá[c,*]

[a] *Grup d'Enginyeria Molecular, Institut Químic de Sarrià, Universitat Ramon Llull, Vía Augusta 390, 08017-Barcelona, Spain.*

[b] *Departamento de Biología, Facultad de Ciencias, Universidad Autónoma de Madrid, Darwin 2, Cantoblanco, 28049-Madrid, Spain.*

[c] *Departament de Bioquímica i Biologia Molecular, Facultat de Biologia, Universitat de Barcelona, Avinguda Diagonal 645, 08028-Barcelona, Spain.*

** Corresponding author. Departament de Bioquímica i Biología Molecular, Facultat de Biologia, Universitat de Barcelona, Avinguda Diagonal 645, 08028-Barcelona, Spain. Tel.: +34 934 02 12 12, fax: +34 934 02 15 59.*

E-mail address: mlsagrista@ub.edu

Do folate-receptor targeted liposomal photosensitizers enhance photodynamic therapy selectivity?

Abstract

One of the current goals in photodynamic therapy research is to enhance the selective targeting of tumor cells in order to minimize the risk and the extension of unwanted side-effects caused by normal cell damage. Special attention is given to receptor mediated delivery systems, in particular, to those targeted to folate receptor. Incorporation of a model photosensitizer (ZnTPP) into a folate-targeted liposomal formulation has been shown to lead an uptake by HeLa cells (folate receptor positive cells) 2-fold higher than the non-targeted formulation. As a result, the photocytotoxicity induced by folate-targeted liposomes was improved. This selectivity was completely inhibited with an excess of folic acid present in the cell culture media. Moreover, A549 cells (folate receptor deficient cells) have not shown variations in the liposomal incorporation. Nevertheless, the differences observed were slighter than expected. Both folate-targeted and non-targeted liposomes localize in acidic lysosomes, which confirms that the non-specific adsorptive pathway is also involved. These results are consistent with the singlet oxygen kinetics measured in living cells treated with both liposomal formulations.

Keywords

Photodynamic therapy, folate receptor, liposomes, targeted drug delivery, singlet oxygen.

Abbreviations

BCA, bicinchoninic acid; DMEM, Dulbecco´s Modified Eagle´s Medium; DMSO, dimethyl sulfoxide; D-PBS, deuterated phosphate-buffered saline; FA-PEG-DSPE, 2-distearoyl-*sn*-glycero-3-phosphoethanolamine-N-[folate(polyethylene glycol)-2000] (ammonium salt); FBS, fetal bovine serum; FD-DMEM, folate-deficient Dulbecco´s Modified Eagle´s Medium; MLV, multilamellar vesicle; MTT, 3-[4,5-dimethylthiazol-2-yl]-2,5-diphenyltetrazolium bromide; OOPS, 1,2-dioleoyl-*sn*-glycero-3-[phospho-*L*-serine] (sodium salt); PBS, phosphate-buffered saline; PDT, photodynamic therapy; POPC, 1-palmitoyl-2-oleoyl-*sn*-glycero-3-phosphocholine; PS, photosensitizer; SDS, sodium dodecyl sulfate; THF, tetrahydrofuran; ZnTPP, 5,10,15,20-tetraphenyl-21*H*,23*H*-porphine zinc.

1. Introduction

Photodynamic therapy (PDT) is an emerging modality for the treatment of various ophthalmic, dermatologic, cardiovascular, and predominantly, oncologic diseases, that involves light, a photosensitizer (PS) and tissue oxygen, all innocuous for the cells by themselves [1-4]. The combined action of the triplet state of the PS and molecular oxygen results in the formation of singlet oxygen ($^1O_2$) a reactive oxygen species (ROS) which is thought to be the main responsible of photo-induced cell death, playing a key role in both apoptotic and necrotic pathways [5-7]. Once produced, $^1O_2$ may diffuse away from the site of production; oxidize biomolecules encountered along its path, or decay back to the ground state within its lifetime. The tiny fraction of $^1O_2$ which undergoes radiative decay emitting at 1280 nm is employed for optical $^1O_2$ detection. The time-resolved measurement of this emission is a very well-established method for monitoring $^1O_2$ production and determining its lifetime [8, 9].

One of the most actively pursued goals in PDT research is to enhance the selective targeting of tumor cells in order to minimize the risk and extension of unwanted side-effects caused by damage to normal tissues [10]. Targeted drug delivery systems are one of the strategies proposed to solve the problems underlying traditional cancer treatments. Drug delivery systems are able to modify the pharmacokinetics and biodistribution of their associated drugs. In this way, liposomes possess many interesting properties such as the ability to entrap both hydrophilic and hydrophobic drug molecules without loss or alteration of their activity, long systemic circulation times, preferential accumulation in solid tumors, and controlled drug release [11-13]. In PDT, it has been shown that liposomes increase the photosensitizing efficiency of some PDT agents by maintaining their monomeric form, by modifying the uptake of the dye by malignant cells, or by influencing their subcellular accumulation [14, 15].

One approach to improve the therapeutic efficacy of drug-carrying liposomes is the grafting of tumor-specific ligands to their lipid bilayer, which can be recognized by specific cell surface components [16], e.g., antibodies [17], growth factors [18], glycoproteins (transferrin) [19], or specific receptors [20]. The incorporation of ligand-targeted therapies not only facilitates targeting to the cell but also drug retention at the target site by preventing the rapid elimination from the system circulation. These ligands represent a minimal risk of inducing immune response, are widely available and often inexpensive. At present, special attention is given to folate receptor (FR)-mediated delivery systems [21]. Folic acid is an essential vitamin for the proliferation and maintenance of all cells. The lack of this nutrient in human serum makes malignant cells to up-regulate this receptor to compete more aggressively for the vitamin. The overexpression of folate receptor on a variety of epithelial cancer cells including cancers of ovary, lung, kidney, breast, brain and colon [22], and the extremely high affinity of folate for its receptor provide a novel approach to specifically deliver PSs encapsulated in folate-functionalized liposomes *in vitro* [23]. Improved uptake of PS-folate conjugates has been reported previously [24, 25] and different systemic carrier platforms have been developed to achieve selective accumulation of PSs [26-30]. However, the details of such improved PS uptake are poorly understood. For instance, to what extent does receptor-mediated uptake affect the accumulation of PSs in the cells? Does receptor-mediated uptake affect the localization of the PSs in the cells? Are the photosensitization properties affected?

In order to address these questions, the model PS zinc-tetraphenylporphyrin (ZnTPP) was encapsulated in folate-targeted and non-targeted liposomes to assess the role of folate receptors in the active uptake of folate-targeted liposomes. ZnTPP was chosen as PS as it can be conveniently encapsulated in liposomes in high yield and in monomeric state [31, 32]. Our results show that targeting HeLa cells (FR-overexpressing cervical carcinoma cell line) with folate-decorated liposomes indeed

leads to an increased PS uptake. This enhancement induces higher photodynamic cell death compared to that caused by incubation with non-targeted liposomes. We subsequently describe a comparative study of accumulation and phototoxicity in FR-expressing HeLa tumor cells, and in A549 tumor cells which do not express FR. Subcellular localization patterns of both formulations were studied, as well as $^1O_2$ kinetics measured in living cells.

2. Materials and methods

2.1. Chemicals

1-palmitoyl-2-oleoyl-*sn*-glycero-3-phosphocholine (POPC), 1,2-dioleoyl-*sn*-glycero-3-[phospho-*L*-serine] (sodium salt) (OOPS) and 1,2-distearoyl-*sn*-glycero-3-phosphoethanolamine-N-[folate(polyethylene glycol)-2000] (ammonium salt) (FA-PEG-DSPE) were purchased from Avanti Polar Lipids (Birmingham, AL, USA). Imidazole, folic acid and 5,10,15,20-tetraphenyl-21*H*,23*H*-porphine zinc (ZnTPP) was purchased from Sigma-Aldrich Chemical Co. (St. Louis, MO, USA) The porphyrin used had a minimal purity of 99% and was used as received. Deuterium oxide (99.9%) was purchased from Solvents Documentation Synthesis (SDS, Peypin, France). All other chemicals were commercially available reagents of at least analytical grade. Milli-Q water (Millipore Bedford, Massachusetts system, resistivity of 18 MΩ cm) was used.

Dulbecco´s Modified Eagle´s Medium (DMEM) with 4.5 g/L glucose, folate-deficient DMEM with 4.5 g/L glucose (FD-DMEM), fetal bovine serum (FBS), penicillin-streptomycin solution and *L*-glutamine solution for biological assays were purchased from Biological Industries (Kibbutz Beit Haemek, Israel). Sterile Dulbecco's phosphate-buffered saline (PBS) and 3-[4,5-dimethylthiazol-2-yl]-2,5-diphenyltetrazolium bromide (MTT) were purchased from Sigma-Aldrich. MicroBCA protein assay kit was purchased

from Pierce Protein Research Products (Rockford, IL, USA) and used according to the product information sheet. The sterilized material was purchased from Techno Plastic Products (Trasadingen, Switzerland).

2.2. Cell cultures

Human HeLa cervical adenocarcinoma cell line (ATCC CCL-2) is one of many tumor cell types that are known to over-express folate receptors [33]. Human lung adenocarcinoma A549 cells (ATCC CCL-185), known to be deficient in FR expression, were used as negative control. HeLa and A549 cells are adherent cells which grow up to form cellular monolayers toward confluence after seeding. These cells were cultured at 37 ºC in a humidified sterile atmosphere of 95% air and 5% CO_2, using DMEM supplemented with fetal bovine serum (10% v/v), glucose (4.5 g/L), *L*-glutamine (292 mg/L), streptomycin sulfate (10 mg/L) and potassium penicillin (10000 U/L). Before the experiments the cells were subcultured in folate-deficient DMEM (FD-DMEM) supplemented with the same components as DMEM for 2 weeks to establish a folate deficiency. Cell lines were maintained frozen in DMEM with 10% DMSO. 1.8 mL CryoTubes™ (Nunc, Nalge Nunc International, IL, USA) were filled with the cell suspension and placed in a cell Cryo 1 ºC Freezing Container (Nalgene, Nalge Nunc International, IL, USA) to be slowly frozen up to -80 ºC at a cooling rate of -1 ºC/min for successful cell cryopreservation. Frozen cells were rapidly transferred to a liquid nitrogen container (-196 ºC) and stored.

2.3. Preparation of liposomes

Folate-targeted and non-targeted liposomes for porphyrin incorporation were prepared by microemulsification following standard procedures [31, 32]. Briefly,

POPC/OOPS (90:10 molar ratio, non-targeted liposomes) and POPC/OOPS/FA-PEG-DSPE (90:10:0.1 molar ratio, FR-targeted liposomes) mixtures containing the photosensitizer ZnTPP at 100:1 lipid/porphyrin molar ratio were evaporated to dryness from a chloroform solution and kept in a vacuum desiccator for 12 h over P_2O_5 in order to remove the last traces of the solvent. Multilamellar vesicles (MLVs) were prepared by hydratation of the dried lipid films by vortexing for 30 min (alternating 30 s periods of heating and 30 s of vortexing) at a concentration of 20 mg lipid/mL of 50 mM imidazole-HCl buffer (pH 7.4) at 45 ºC. The MLVs dispersion was frozen and thawed (five times), sonicated (bath sonicator, 15 min, 45 ºC) and microemulsified (EmulsiFlex B3 device, Avestin, Ottawa, Canada). Microemulsification was carried out by pumping the fluid fifteen times through the interaction chamber (45 ºC, 200 kPa). Control liposomes were prepared in the same way but without the PS. The liposomes were stored in the dark at 4 ºC. Subsequent liposome handling procedures were all performed in the dark.

2.4. Liposome characterization

The PS and the lipid content in the liposomes were evaluated following standard procedures. Liposomes were disrupted by the addition of THF to an aliquot of the liposomal suspension, free of non-entrapped PS, obtained in imidazole-HCl buffer (THF/imidazole-HCl buffer, 24/1, v/v) and the absorbance was measured at λ_{max} of the Soret band. The PS concentration was determined by comparison with standard curves obtained in the same conditions. Lipid content was quantified by a colorimetric assay with ammonium ferrothiocyanate according to the method of Stewart [34]. The average size and polydispersity of unilamellar vesicles and the zeta potential were determined by photon correlation spectroscopy (PCS). A Zetasizer Nano-ZS (Malvern Instruments, UK) and a 4 mW He-Ne laser (Spectra Physics), at an excitation wavelength of 633 nm, were used. Before measuring, samples were appropriately diluted to avoid multiple

scattering. To control the stability of the formulations, the PS and lipid content in liposomes as well as the average size and polydispersity of the vesicles were also determined after storage up to 7 days.

The stability of liposomes was also tested in presence of 10% FBS following the procedure described in [35]. Liposomal suspensions containing ZnTPP with a final concentration of 10 μM were incubated in imidazole-HCl buffer with 10% FBS at 37ºC with continuous stirring for different periods of time up to 48 h. After each incubation period, 200 μL of the mixtures were withdrawn and centrifuged at 4000 rpm to eliminate any non-encapsulated PS, appeared as a result of the disruption of the liposomes due to its interaction with serum components. Then, 1.5 mL of THF were added to 50 μL of each supernatant to disrupt the liposomes, liberating the porphyrin still encapsulated in the liposomes and precipitating the serum components. These samples were centrifuged at 4000 rpm to obtain a clear supernatant and the absorption spectra were recorded.

2.5. Dark toxicity and cell uptake

To select the ZnTPP concentration in cell cultures for uptake experiments, the PS dark toxicity was determined after incubation with 1 - 50 μM ZnTPP for up to 24 h. Cell viability was evaluated 24 h after treatment by the MTT colorimetric assay [36]. Briefly, after washing with PBS, DMEM containing 0.5 mg/mL MTT was added and incubated for 1 h at 37 ºC. The medium was replaced by DMSO and the absorbance at 550 nm was read on a Bio-Rad Benchmark Plus microplate reader.

A concentration of 10 μM ZnTPP was chosen as a good compromise between cell viability and PS concentration in culture medium, with survivals fractions higher than 85% for non-targeted and folate-targeted formulations, for both cell lines. The

cellular uptake of ZnTPP was determined by fluorescence spectroscopy. HeLa and A549 cells were seeded in 25 cm^2 tissue culture flasks and grown toward 80-85% confluence in FD-DMEM. Cells were incubated in the dark with the appropriate volume of the folate-deficient medium containing 10 μM ZnTPP encapsulated in the two different liposomal formulations, for different times ranging from 30 min to 24 h. In free folate competition studies, 1 mM folic acid was added to the incubation medium. Afterwards, the medium was discarded and the cells were washed three times with PBS, scrapped and resuspended in 1 mL of 2% sodium dodecyl sulphate (SDS) in Milli-Q water. The resulting suspension was centrifuged at 10,000 rpm for 10 min (Sigma 2-16P centrifuge, angle rotor 24x1.5/2.2 mL). The extent of PS uptake was assessed by comparison between the fluorescence of this supernatant to that of standard solutions under the same conditions. The fluorescence intensity values obtained for each sample were normalized to the number of cells determined by the bicinchoninic acid (BCA) protein assay [37]. Each experiment was repeated twice.

In order to study the liposome cell internalization [38] and to distinguish surface bound to internalized liposomes, HeLa cells were incubated either at 4ºC (where folate-receptor-mediated endocytosis is blocked [23, 39]) or 37ºC in the dark for 4 h with FD-DMEM containing 10 μM ZnTPP encapsulated in non-targeted and FR-targeted liposomes. Since folate rapidly dissociates from specific, high-affinity binding factors in acid pH [40], we used an acidic saline wash to remove surface-bound liposomes and distinguish the uptake due to surface binding than that due to internalization. After rising with PBS, cells were incubated for 10 min with acetate buffer pH 3.5 (130 mM NaCl, 20 mM NaAc). Cells were then scrapped and resuspended in 1 mL of 2% SDS. The extent of PS uptake was assessed by the same procedure described above.

2.6. Subcellular localization and quantitative analysis

Folate-deficient HeLa cells were grown on 22 mm square coverslips placed into 35 mm culture dishes. They were incubated at 37 ºC for 24 or 48 h with FD-DMEM containing 1 or 10 μM ZnTPP encapsulated in folate-targeted or non-targeted liposomes. Cells were washed four times with PBS, mounted in DMEM and observed immediately. Microscopic observations and photography were performed with a Leica TCS SP2 confocal microscope (Wetzlar, Germany), operating with the 561 nm laser line. To confirm the intracellular localization of ZnTPP, the endocytic compartments of the HeLa cells were labeled with the fluoroprobe LysoTracker Red DND-99 (200 nM, Molecular Probes, Eugene, OR) or MitoTracker Deep Red (50 nM, Molecular Probes, Eugene, OR) in the culture medium at 37ºC for 30 min. After labeling, the coverslips were washed with PBS and observed in a microscope under green excitation filter to detect the emission of LysoTracker or MitoTracker. Microscopy and photography of control cells were performed using a BX61 epifluorescence microscope (Olympus, Tokyo, Japan). Photographs were processed using Adobe Photoshop CS2 software (Adobe Systems, San Jose, CA). Quantitative studies on HeLa cells subjected to 1 or 10 μM ZnTPP in liposomes with and without folate were carried out using image processing and analysis (IPA) from the public domain ImageJ 1.42 software (http://rsbweb.nih.gov/ij/index.html) [41]. The red ZnTPP signal was recorded for each cell, brightness values in arbitrary units corresponding to the following ratio: integrated density/area. Results were the mean values and standard deviations from a total of 70 images. In addition, the frequency of brightness values (red signal) was also evaluated for cells subjected to 24 h treatments with 1 or 10 μM ZnTPP in liposomes either with or without folate.

2.7. Photodynamic treatment *in vitro*

Folate-deficient cells were seeded in 96-well plates and cultured towards 80-85% confluence. They were then incubated in the dark at 37 ºC with FD-DMEM containing 0.1 - 10 μM ZnTPP encapsulated in the two different liposomal formulations. After 24 h incubation, cells were washed three times with PBS and replenish with fresh FD-DMEM. Irradiation was carried out with a Sorisa Photocare LED source with a wavelength range of 520-550 nm. The light intensity at the irradiation site was 16 mW/cm^2, measured with a LaserStar Ophir power meter (Logan, UT, USA). Cells were irradiated for different times ranging from 2 min to 30 min and then incubated for 24 h before the MTT assay for cell viability. Experiments were performed in triplicate.

2.8. Spectroscopic measurements

Absorption spectra were recorded on a Varian Cary 4E spectrophotometer, equipped with a 110 mm-diameter integrating sphere for transmittance measurements. Fluorescence emission and excitation spectra were recorded in a Jobin-Ybon Specx Fluoromax-2 spectrofluorometer. The fluorescence quantum yields were determined by comparison of the areas under the emission curves for optically-matched suspension of liposomes and a reference, after correcting for the refractive index of the solvent. ZnTPP in toluene was used as reference with Φ_F=0.033 [42]. Fluorescence decays were recorded in a time-correlated single photon counting system (Fluotime 200, PicoQuant GmbH, Berlin, Germany) with a 596-nm excitation LED. The fluorescence decays were analyzed using the PicoQuant FluoFit 4.0 data analysis software.

[1]O_2 phosphorescence was detected using a customized PicoQuant Fluotime 200 system described elsewhere [43, 44]. Briefly, a diode-pumped pulsed Nd:YAG laser (FTSS355-Q, Crystal Laser, Berlin, Germany) working at 10 kHz repetition rate at 532 nm (12 mW, 1.2 μJ per pulse) was used for excitation. A 1064 nm rugate notch filter (Edmund Optics, UK) was placed at the exit port of the laser to remove any residual component of its fundamental emission in the near-IR region. The luminescence exiting from the side of the cuvette was filtered by a cold mirror (CVI Melles Griot, USA) to remove any scattered laser radiation. A TE-cooled Hamammatsu near IR photomultiplier (model H9170-45), sensitive from 950 to 1400 nm, was used to detect the $^1O_2$ phosphorescence. The detector was operated in photon counting mode and its output sent to a multichannel scaler PicoQuant Nanoharp 250.

Transient absorption spectra were measured by nanosecond laser flash photolysis using a Q-switched Nd-YAG laser (Surelite I-10, Continuum) with right-angle geometry and an analysing beam produced by a Xe lamp (PTI, 75 W) in combination with a dual-grating monochromator (mod. 101, PTI) coupled to a photomultiplier (Hamamatsu R928). Kinetic analysis of the individual transients was achieved with the FitLW software developed in our laboratory.

For spectroscopic measurements in cell suspensions HeLa cells were incubated in the dark with 10 μM ZnTPP encapsulated in folate-targeted and non-targeted liposomes for 24 h. The medium was discarded and the cells were washed three times with PBS, scrapped and resuspended in 1.5 mL of PBS or D_2O-based PBS (D-PBS). The samples contained about 8 millions of cells in 1.5 mL of PBS and were continuously stirred during the measurements. The measurements were then carried out within the following 45 min.

All spectroscopic measurements were carried out in 1-cm quartz cuvettes (Hellma, Germany), at room temperature and under continuous stirring.

2.9. Statistical analysis

Unpaired Student's *t* test was used to test for the significance level between two sets of measurements. The level of significance was set to $p < 0.05$.

3. Results and Discussion

3.1. Characterization of liposomal formulations.

FR-targeted and non-targeted liposomes containing ZnTPP at 100:1 lipid/porphyrin molar ratio were prepared by microemulsification. This particular combination of PS and lipids allows for a high encapsulation of this PS [31]. The PS encapsulation efficacy was close to 90% and was not affected by folate functionalization. Photon Correlation Spectroscopy (PCS) showed a dynamic diameter of 110 nm for non-targeted liposomes and 140 nm for FR-targeted liposomes with a polydispersity index of 0.3. The stability of the formulations was monitored by changes in the particle size and porphyrin and lipid retention over one week storage at 4 ºC in the dark (Table 1). The liposomal formulations showed excellent colloidal stability and drug retention during this period. We thus conclude that the properties and stability of liposomal preparations are not affected by the presence of the folate marker.

The phase transition temperature of POPC/OOPS (90:10) liposomes was reported previously as -5.1 ± 0.7 ºC and was not affected by the incorporation of 1% ZnTPP [31]. Thus, one can reasonably expect that it wont' be affected either by the

presence of 0.1 mol% FA-PEG-DSPE. The liposomes can therefore be safely assumed to be in the fluid state at 37 ºC, temperature at which cell experiments were carried out. In order to ensure that ZnTPP does not escape from liposomes interacting with serum proteins, the stability of liposomes was tested also in the presence of 10% FBS at 37ºC. The remaining PS in both FR-targeted and non-targeted liposomal suspensions was always above 90%, indicating that serum proteins do not affect liposome stability and, especially, do not induce the release of the entrapped ZnTPP.

PLEASE INSERT TABLE 1 HERE

The same holds true for the photophysical properties of the sensitizer: Fig. 1 shows the absorption and emission spectra of ZnTPP encapsulated in folate-targeted liposomes and their non-targeted counterparts. No spectral shifts can be observed between the two sets of data, ruling out any significant interaction of the porphyrin with the folate ligand. Likewise, the fluorescence quantum yield of ZnTPP, calculated by steady-state comparative method of optically-matched solutions, was 0.025 and 0.024 for folate-targeted liposomes and non-targeted liposomes, respectively ($\Phi_{F\ (ZnTPP,\ toluene)}$ = 0.033) [42]. Finally, the fluorescence decay kinetics, determined by time-correlated single photon counting, also confirmed that the photophysics of ZnTPP in the lipid bilayers are not affected by the presence of the FA-PEG-DSPE ligand. The fluorescence decay could be fitted in both systems by two exponential components with lifetimes 2.0 ± 0.1 and 1.3 ± 0.1 ns, respectively, reflecting different endoliposomal locations of ZnTPP in the phospholipid bilayer [45].

PLEASE INSERT FIGURE 1 HERE

3.2. Cellular uptake of FR-targeted liposomes.

After confirming that ZnTPP incorporation into the lipid bilayers is not affected by the presence of the FA-PEG-DSPE ligand, the effect of the folate marker on the cellular uptake of ZnTPP was determined. HeLa and A549 cells were incubated for different times with 10 μM ZnTPP encapsulated in folate-targeted and non-targeted liposomes. The extent of PS uptake was then determined by fluorescence spectroscopy after lysing the cells and then normalized to the protein content of each sample to correct for variations in the number of cells. As shown in Fig. 2A, a clear differential uptake between folate-targeted and non-targeted liposomes was observed. Thus, when FR-overexpressing HeLa cells were incubated for 24 h with folate-targeted liposomes, a 70% increase of lysate fluorescence is observed compared to the values for non-targeted liposomes. Moreover, FR-deficient A549 cells showed no differences in the liposomal incorporation (Fig. 2B). These results confirm that active uptake mediated by folate receptors is an effective approach to increase the uptake of PS encapsulated in folate-functionalized liposomes.

PLEASE INSERT FIGURE 2 HERE

Additional evidence for the specific role of folate-receptor interactions in the differential uptake of ZnTPP was obtained from competitive binding assays. Thus, 1 mM folic acid was added to the incubation medium to saturate the receptors on the cell surface. Fig. 3 shows that 1 mM free folic acid significantly reduced the ZnTPP uptake in HeLa cells targeted with liposomes bearing folate ligands and no differences were observed between targeted and non-targeted liposomes uptake, indicating that the contribution of folate receptors to the uptake of ZnTPP was completely inhibited.

PLEASE INSERT FIGURE 3 HERE

In a third series of experiments, the effect of FA-PEG-DSPE liposomal content on the uptake of ZnTPP was also assessed. HeLa cells were incubated for 24 h with different formulations containing 0 - 0.2 mol% of FA-PEG-DSPE and the fluorescence of the cell lysate was measured and normalized to the protein content of each sample. As expected, uptake of ZnTPP was found to be notably dependent on the amount of FA-PEG-DSPE present in the liposomes (Fig. 4). Increasing amounts of the folate ligand led to higher uptake of the PS although saturation effects were observed at the highest FA-PEG-DSPE concentration assayed. Since FR can bind only one molecule of folic acid [40], we chose to use 0.1 mol% FA-PEG-DSPE in all experiments, which also precludes the formation of folate dimers and trimers [46]. . Thus, we can ensure an efficient interaction with folate receptors.

PLEASE INSERT FIGURE 4 HERE

To check whether the incubation at 4°C prevents ZnTPP uptake, the cell-surface binding capacity of folate-targeted and non-targeted liposomes was estimated from the differential uptake of ZnTPP by HeLa cells incubated at 4ºC or 37ºC (Fig. 5). In both cases, the extent of PS uptake was dramatically reduced when the incubation of ZnTTP-containing liposomes was performed at 4ºC, suggesting that endocytosis is the main cell internalization mechanism. Moreover, at this low temperature, almost a two-fold increase of cell-lysate fluorescence was observed for folate-targeted liposomes compared to non-targeted ones. This indicates that the differential uptake between folate-targeted and non-targeted liposomes is amplified due to enhanced surface binding of the former. Nevertheless, an acidic wash of the cells caused the release of surface-bound folate-targeted liposomes, showing that the uptake due to binding to the folate receptor was greatly diminished under such acidic conditions [23, 39, 40].

PLEASE INSERT FIGURE 5 HERE

Taking all these results together, the preferential uptake of folate-targeted liposomes was demonstrated in HeLa cells. Nevertheless, the differences observed were smaller than expected [23, 47, 48]. Moreover, non-targeted liposomes are also internalized, revealing that non-specific endocytosis also contribute to the uptake. Qualls and Thompson [26] also observed non-specific liposomal uptake pathways when KB cells, also overexpressing folate receptors [24], were treated with $AlPcS_4^{4-}$ encapsulated in folate-displasmenylcholine liposomes.

3.3. Photosensitization experiments.

Studies on the efficiency of the FR-targeted liposomes for PDT are summarized in Figs. 6 and 7. A549 and HeLa cells were incubated in the dark with different concentrations of ZnTPP entrapped in FR-targeted and non-targeted liposomes for 24 h prior to photosensitization. Afterwards, cells were exposed to green light using a LED source. Cell survival was assessed by MTT assay 24 h after treatment. Dark cytotoxicity experiments yielding survival cell fraction higher than 85% demonstrated that incubation with FR-targeted and non-targeted liposomes at the concentrations used did not induce significant cell death without irradiation. Fig. 6 shows the light and concentration dependence of the photodynamic response of HeLa cells for both types of ZnTPP-loaded liposomes. As expected, increasing the light dose and the concentration of the PS led to enhanced photocytotoxicity. Folate-decorated liposomes consistently led to higher photosensitivity of the cells. Irradiation of cell cultures alone or incubated with empty liposomes did not induce any toxicity.

PLEASE INSERT FIGURE 6 HERE

A better appreciation of the folate-labeling effects can be gained by comparing the photodynamic effect under the same conditions. Thus, for 1 μM ZnTPP incubated for 24 h in A549 and HeLa cells and irradiated with 10 J·cm^{-2} (Fig. 7), non-targeted liposomes caused 65 ± 5% cell death in both cell lines. The use of FR-targeted liposomes increased the cell mortality to 94 ± 5% for FR-positive HeLa cells, while it remained at 60 ± 5% for FR-negative A549 cells. Thus folate-targeted liposomes enhanced cell mortality by 50% in FR-positive HeLa cells.

PLEASE INSERT FIGURE 7 HERE

3.4. Subcellular localization

Fluorescence and differential interference contrast images of HeLa cells after 24 or 48 h incubation with folate-targeted and non-targeted liposomes (10 μM ZnTPP bulk concentration) are shown in Fig. 8. The cells displayed a pattern of intense granular signal in the cytoplasm. The site of ZnTPP accumulation strongly resembled that of acidic organelles and therefore, lysosomes could be the main site of ZnTPP accumulation. Additionally, the intracellular localization of ZnTPP was compared with the distribution of fluorescent probes specific to lysosomes (LysoTracker Red) and to mitochondria (MitoTracker Red). LysoTracker and Mitotracker Red probes are commonly used in several research areas, including PDT studies [49-52]. As shown in Fig. 8A, the intracellular distribution of ZnTPP was clearly similar to LysoTracker Red, and clearly different from the mitochondrial network displayed with MitoTracker Red, under green excitation epifluorescence microscopy. We could not observe the co-localization of ZnTPP and LysoTracker probe because of the red emission of both dyes. The intensity of the punctate fluorescence was dependent on the porphyrin concentration, incubation time, as well as ZnTPP liposomal formulation. It is important to note that no morphological changes were detected in the cells under these conditions and no relocalization of the PS was observed when cells were exposed to prolonged exciting light. Non-specific adsorptive endocytosis pathway was confirmed by the fact that the intracellular localization of ZnTPP from by non-targeted liposomes was identical to that of liposomes with folate.

Cells treated with 10 μM ZnTPP vehiculizated in liposomes with folate appeared with a higher fluorescence signal in relation to folate-free liposomes (see Fig. 8A).

These results were confirmed by the quantitative analysis of fluorescence intensity using ImageJ 1.42 software (Fig. 8B and C), and results are consistent with the cellular uptake measured by cell lysate fluorescence.

PLEASE INSERT FIGURE 8 HERE

3.5. Time-resolved $^1O_2$ detection in HeLa cells incubated with ZnTPP encapsulated in FR-targeted and non-targeted liposomes.

In a typical experiment, 1.5 mL- D_2O-based PBS (D-PBS) cell suspension containing ~ 8 x 10^6 cells incubated with ZnTPP encapsulated in FR-targeted and non-targeted liposomes was assayed for $^1O_2$ using pulsed laser excitation at 532 nm and observing the $^1O_2$ phosphorescence at 1280 nm. Indeed, the samples produced clear $^1O_2$ phosphorescence signals showing the expected rise-and-decay shape (Fig. 9). Kinetic analysis of the data in Fig. 9 yielded lifetimes τ_1 = 1.5 ± 0.4 μs for the rise and τ_2 = 6.0 ± 0.5 μs for the decay, the same results being obtained for both FR-targeted and non-targeted liposomes. Thus, the kinetics of $^1O_2$ production and decay in HeLa cells are not affected by the presence of folate ligands on the surface of the liposomes used for delivery of the ZnTPP, suggesting a similar final localization of the PS, in agreement with the confocal microscopy results.

The inset in Fig. 9A shows the transient absorbance of ^{3}ZnTPP in the cell suspension. Kinetic analysis of this signal yields τ_T = 5 ± 1 μs, which means that τ_Δ = 1.5 ± 0.4 μs in HeLa cells. This lifetime is much shorter than the typical value in D_2O (60-70 μs, [53])

indicating that $^1O_2$ is substantially quenched in these cells. Given diffusion coefficients of singlet oxygen in the 0.4 - 2 x 10^{-5} cm^2 s^{-1} range [54-56] and the typical size of the lysosomes (50-500 nm), it can be safely concluded that primary $^1O_2$ damage will be confined to this organelle, as found previously in human skin fibroblasts ([44]). Indeed, we were not able to quench $^1O_2$ with standard quenchers such as sodium azide or bovine serum albumin.

PLEASE INSERT FIGURE 8 HERE

4. Conclusions

A novel folate-targeted liposomal formulation of the model PS ZnTPP has been developed for its selective delivery to FR-overexpressing cancer cells. The stability of liposomal formulations and the photophysical properties of the PS are not affected by the presence of the folate ligand. This folate-targeted formulation shows enhanced ZnTPP internalization and phototoxicity by folate-receptor-positive cells, although non-specific pathways are also involved in cellular uptake. Confocal microscopy and $^1O_2$ kinetics measured in living cells indicate a lysosome localization of ZnTPP in HeLa cells, irrespective of the presence of folate on the liposome surface.

The prevention of liposome uptake at low temperature accounts for the involvement of endocytic pathways in the cellular internalization of both targeted and non-targeted liposomes. Moreover, the reduction of ZnTPP fluorescence in the cells' lysates after an acidic wash confirms the interaction of the folate-targeted liposomes with the receptors. These observations are consistent with the lysosomal localization of ZnTPP.

Taken together, our results suggest that folate ligands enhance the cellular uptake in FR-positive cells mainly as a result of a sustained contact between the liposome and the cell surface, thereby increasing the liposomes' ability to internalize drugs. It will be interesting to see whether in cells with higher FR overexpression this folate-induced selectivity can be further increased. In addition, it will be interesting to study the efficacy of FR-targeted liposomes in preclinical models and their potential for future clinical application in photodynamic therapy.

Acknowledgements

This work was supported by a grant of the Spanish Ministerio de Ciencia e Innovación (CTQ2007-67763-C03/BQU). M.G-D. thanks the Comissionat per a Universitats i Recerca del Departament d'Innovació, Universitats i Empresa de la Generalitat de Catalunya i del Fons Social Europeu for a predoctoral fellowship. We thank Sorisa® (Dr. Albert Amat) for providing us with the Sorisa® Photocare LED source, Dr. Salvador Borrós for Zetasizer Nano-ZS measurements, and Xavier Ragàs for excellent technical assistance.

Table 1. Stability of FR-targeted and non-targeted formulations as measured by lipid and PS content, particle size and zeta potential.

Sample	*Time / h*	*L (%)*[a]	*P (%)*[b]	*Zave / nm*[c]	*ζ pot / mV*[d]
Non-targeted	0	90 ± 2	94 ± 8	110 ± 20	-38 ± 5
	24	97 ± 9	85 ± 10	130 ± 30	-31 ± 3
	168	79 ± 3	83 ± 13	140 ± 20	-30 ± 3
FR-targeted	0	87 ± 4	96 ± 7	140 ± 20	-36 ± 2
	24	97 ± 12	93 ± 4	130 ± 30	-34 ± 2
	168	78 ± 3	83 ± 5	110 ± 20	-35 ± 4

[a] L: Lipid content, expressed as the percentage of lipid in the sample with respect to the lipid present at the initial stage of liposome preparation.

[b] P: Porphyrin content, expressed as the percentage of porphyrin in the sample with respect to the porphyrin present at the initial stage of liposome preparation.

[c] Z average mean.

[d] Zeta potential.

Data are mean values ± SD of at least three independent experiments.

Captions to figures

Figure 1. Absorption (solid line) and emission (dashed line) spectra of ZnTPP incorporated in folate-targeted liposomes (black) and non-targeted liposomes (grey) in 50 mM imidazole-HCl buffer, pH 7.4. Note the factor x10 in the 500-650 nm region of absorption spectra. The spectra were corrected relative to absorption at 550 nm.

Figure 2. Cellular uptake of ZnTPP encapsulated in folate-targeted liposomes (■) and non-targeted liposomes (△) by **(A)** HeLa and **(B)** A549 cells in folate-depleted DMEM media. The fluorescence change plotted is the ratio between the area under the fluorescence emission and the protein content in each suspension. Mean ± SD values from at least two different experiments are shown. ** $p < 0.01$

Figure 3. Competitive binding assay in HeLa cells cultured with FR-targeted and non-targeted liposomes, with or without the addition of 1 mM free folic acid. The enhancement of the FR-targeted liposomes uptake was totally inhibited in the presence of 1 mM free folic acid. Fluorescence emission was normalized with protein content of each suspension. Mean ± SD values from at least two different experiments are shown. **$p < 0.01$.

Figure 4. Uptake of ZnTPP encapsulated in folate-targeted formulations with varying percentages of FA-PEG-DSPE by HeLa cells. Cells were incubated for 24 hours with non-targeted liposomes (0 mol% FA-PEG-DSPE) or folate-targeted liposomes with the FA-PEG-DSPE mole percentage ranging from 0.02 to 0.2. Fluorescence emission was normalized with protein content of each suspension. The fluorescence emission plotted is relative to the lysate fluorescence of cells treated with non-targeted liposomes. The lysate fluorescence corresponding to 0 mol% FA-PEG-DSPE was normalized to 0 ± 12 %. Mean ± SD values from at least three different experiments are shown.

Figure 5. Temperaure-dependent uptake of ZnTPP encapsulated in folate-targeted and non-targeted liposomes. Cells were incubated for 4 hours at 37ºC or 4ºC. The cells were then washed with cold PBS or with acidic saline buffer to remove unattached liposomes or either stripped of surface-bound liposomes. Fluorescence emission was normalized with protein content of each suspension. The fluorescence emission plotted is relative to the mean lysate fluorescence of cells treated with folate-targeted liposomes at 37ºC, normalized to 100 ± 14 %. Mean ± SD values from at least three different experiments are shown.

Figure 6. Concentration and irradiation time dependence of photocytotoxicity of ZnTPP encapsulated in **(A)** non-targeted liposomes and **(B)** folate-targeted liposomes by HeLa cells. The concentrations represented are (●) 0.1 μM , (■) 1 μM and (▲) 10 μM. Mean ± SD from at least three different experiments are shown.

Figure 7. Photodynamic induced citotoxicity of ZnTPP encapsulated in **(A)** non-targeted liposomes and **(B)** folate-targeted liposomes (1 μM, 10 J/cm^2). Mean ± SD from at least three different experiments are shown. ****p < 0.001*

Figure 8. (A) Confocal microscopy images of living HeLa cells incubated 24 or 48 h with different liposomal formulations of 10 μM ZnTPP. (a) and (b) Subcellular localization of ZnTPP in HeLa cells incubated 24 h in liposomes without and with folate, respectively. (c) and (d) Cells displaying the fluorescence pattern of ZnTPP 48 h after incubation in liposomes without and with folate, respectively. All images are the overlay of the fuorescence signal and differential interference contrast (DIC). Scale bar: 10 µm. (e) Localization of MitoTracker Red in HeLa control cells. (f) Localization of LysoTracker Red in HeLa control cells. **(B)** and **(C)** Microscopical evaluation of ZnTPP uptake. B: Mean brightness values (± SD) of the signal from HeLa cells treated for 24 h with 1 or 10 µM ZnTPP in liposomes with (F+) or without (F-) folate. C: Distribution of brightness values from HeLa cells subjected to 24 h treatments with both 1 and 10 µM ZnTPP in liposomes either with or without folate.

Figure 9. Time-resolved luminescence decays of $^1O_2$ recorded at 1280 nm upon 532 nm excitation of a D-PBS HeLa cell suspension, previously incubated with 10 μM ZnTPP encapsulated in (a) non-targeted and (b) folate-targeted liposomes during 24 h in the dark. **A**: fitted parameters: τ_1 = 1.5 ± 0.4 μs, τ_2 = 5.8 ± 0.5 μs ; **Inset A**: ΔAbs signal recorded at 470 nm (triplet absorption), fitted parameters: τ_1 = 5 ± 1 μs; **B**: fitted parameters: τ_1 = 1.5 ± 0.4 μs, τ_2 = 6.1 ± 0.5 μs.

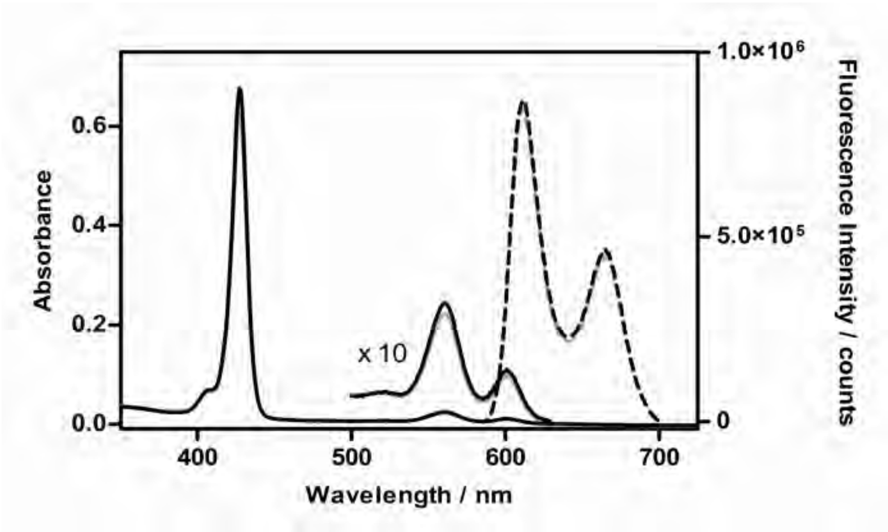

Figure 2

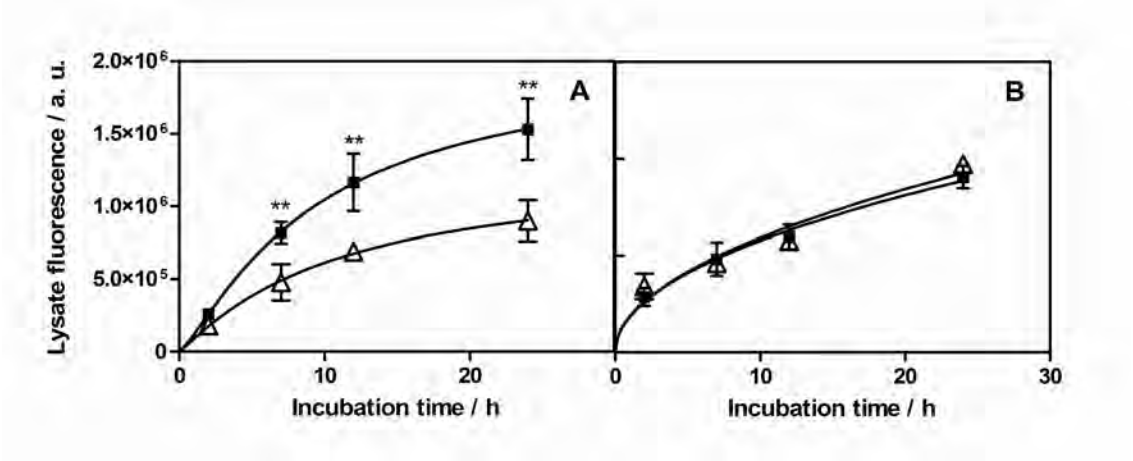

Figure 2

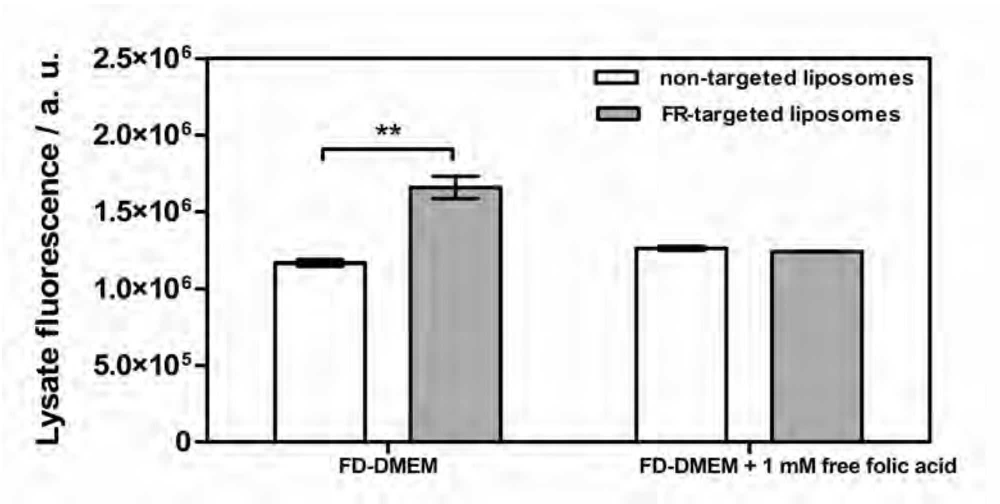

Figure 3

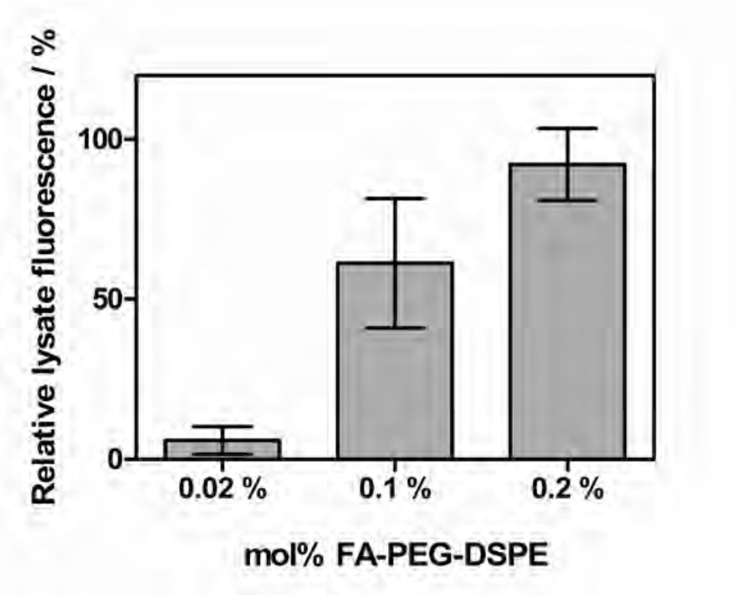

Figure 4

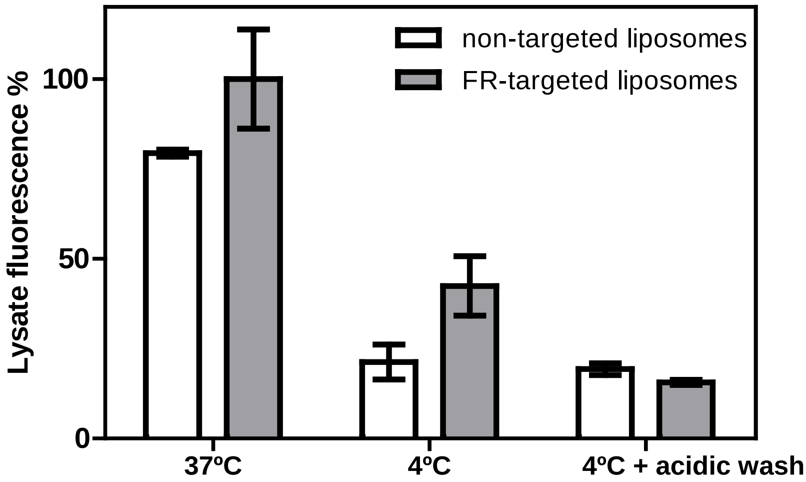

Figure 5

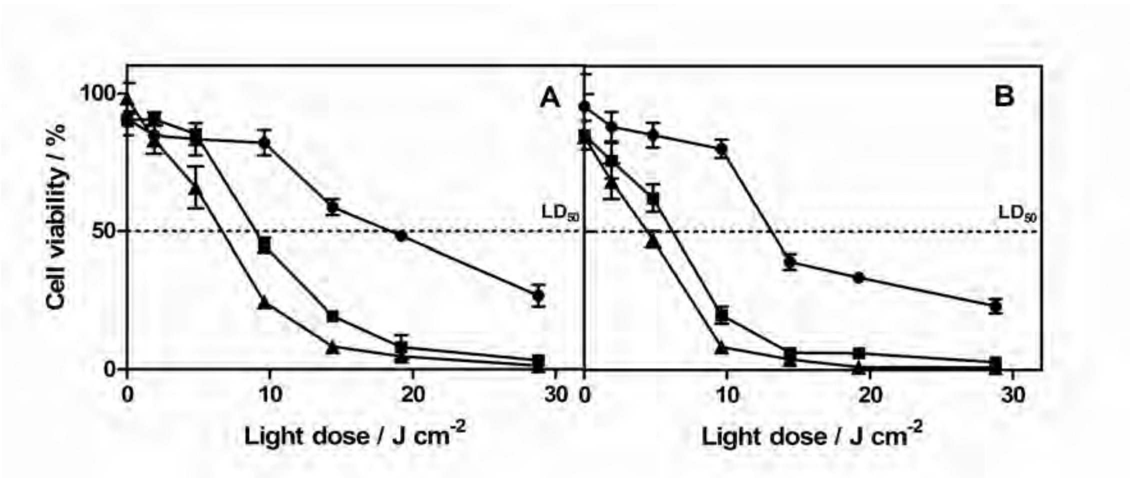

Figure 6

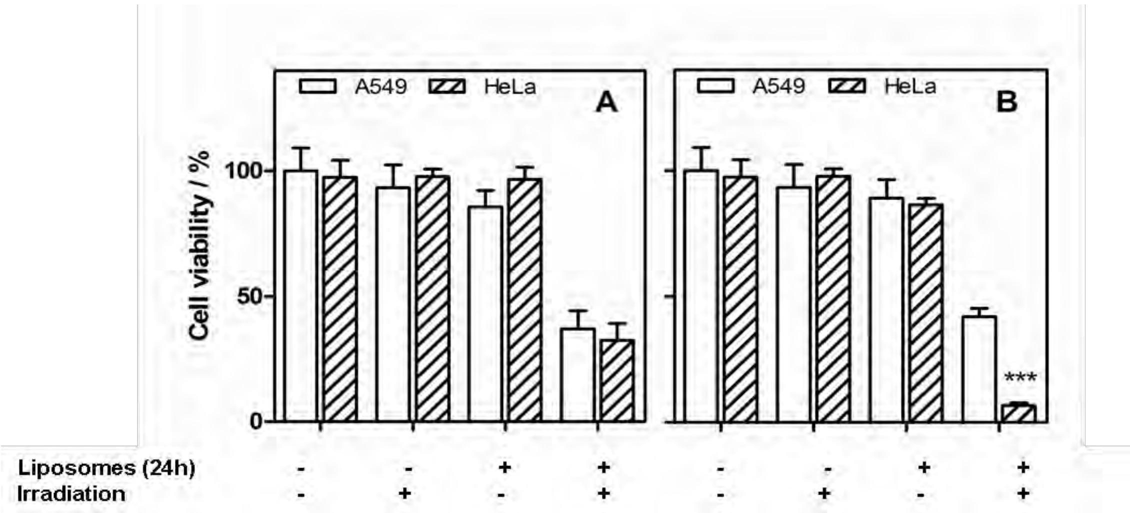

Figure 7

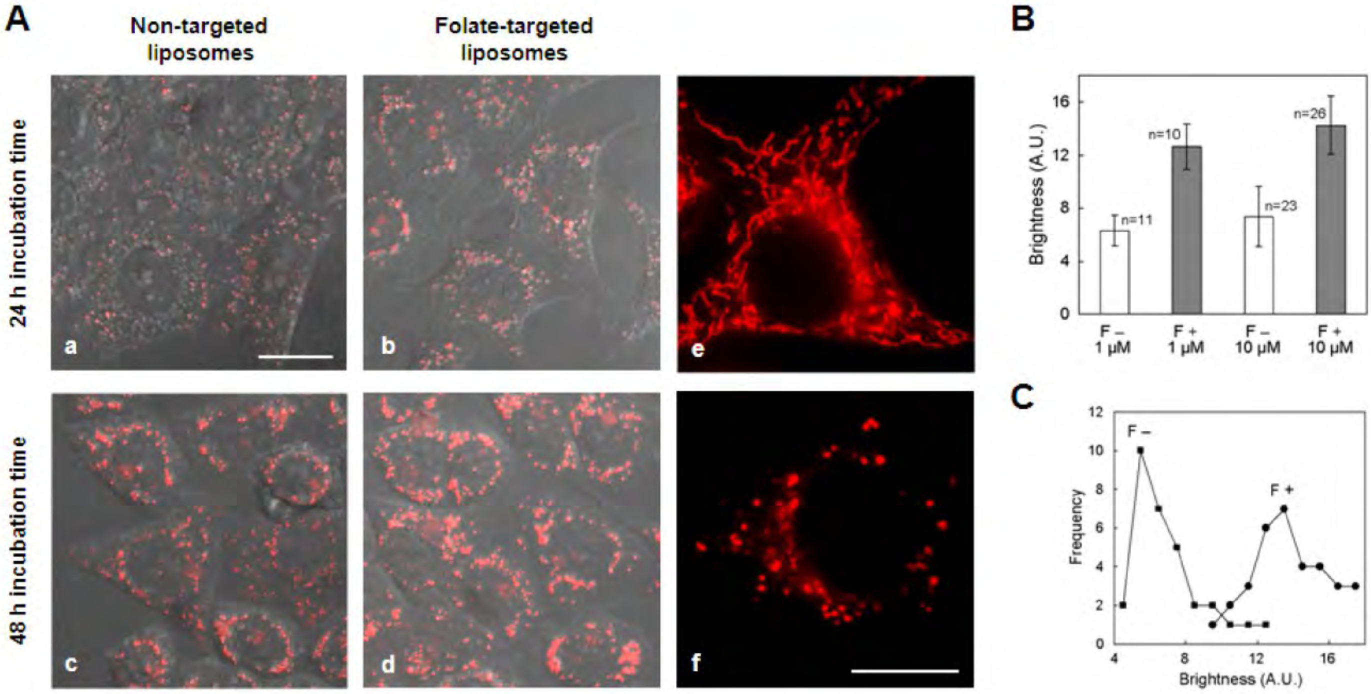

Figure 8

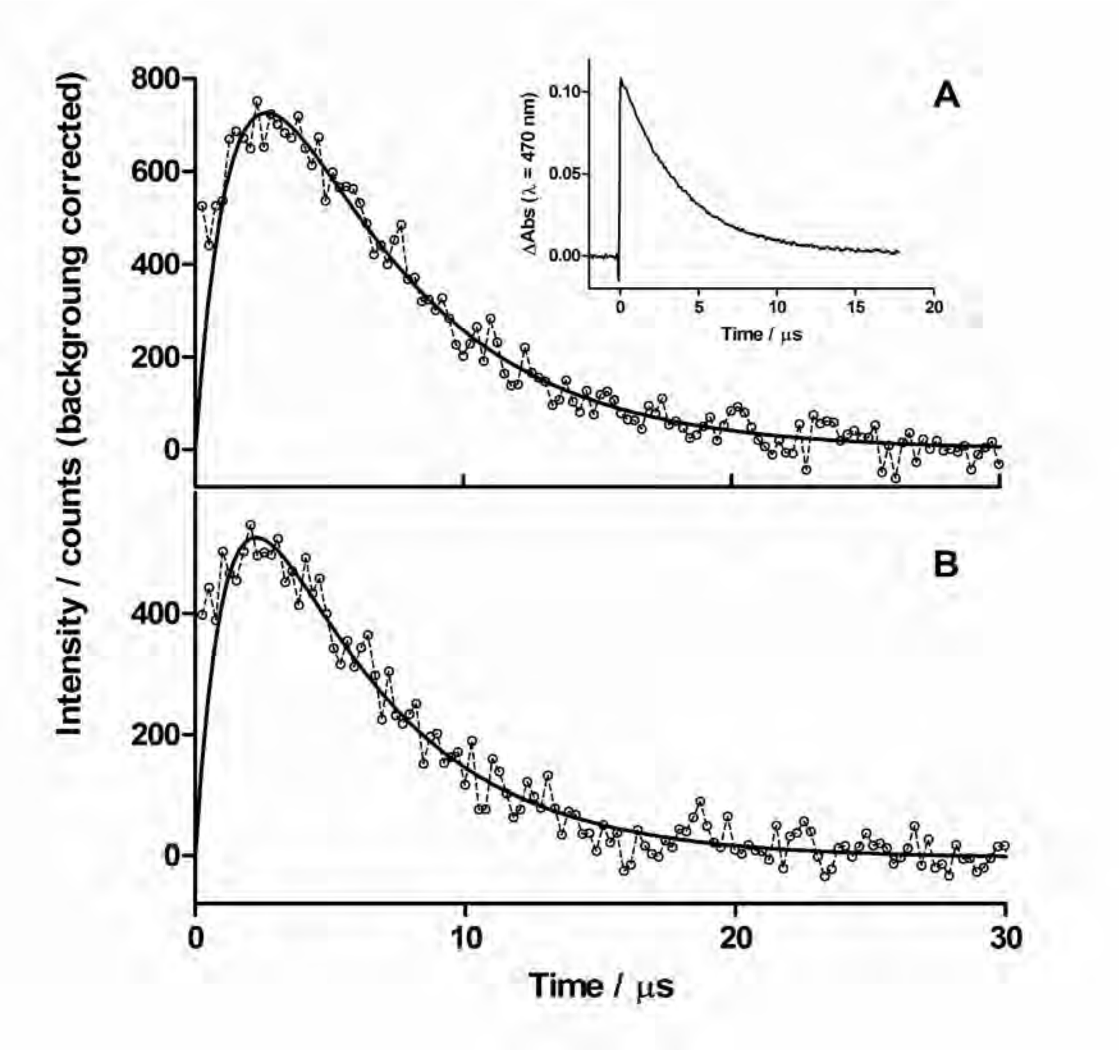

Figure 9

References

[1]B.C. Wilson, M.S. Patterson, The physics, biophysics and technology of photodynamic therapy, Phys. Med. Biol. 53 (2008) R61-109.

[2]M. Ochsner, Photophysical and photobiological processes in the photodynamic therapy of tumours, J. Photochem. Photobiol. B. 39 (1997) 1-18.

[3]S. Choudhary, K. Nouri, M.L. Elsaie, Photodynamic therapy in dermatology: a review, Lasers Med. Sci. 24 (2009) 971-980.

[4]G. Jori, C. Fabris, M. Soncin, S. Ferro, O. Coppellotti, D. Dei, L. Fantetti, G. Chiti, G. Roncucci, Photodynamic therapy in the treatment of microbial infections: basic principles and perspective applications, Lasers Surg. Med. 38 (2006) 468-481.

[5]T.J. Dougherty, C.J. Gomer, B.W. Henderson, G. Jori, D. Kessel, M. Korbelik, J. Moan, Q. Peng, Photodynamic therapy, J. Natl. Cancer Inst. 90 (1998) 889-905.

[6]T.J. Dougherty, An update on photodynamic therapy applications, J. Clin. Laser Med. Surg. 20 (2002) 3-7.

[7]R.W. Redmond, I.E. Kochevar, Spatially resolved cellular responses to singlet oxygen, Photochem. Photobiol. 82 (2006) 1178-1186.

[8]S. Nonell, S.E. Braslavsky, Time-resolved singlet oxygen detection, Methods Enzymol. 319 (2000) 37-49.

[9]C. Schweitzer, R. Schmidt, Physical mechanisms of generation and deactivation of singlet oxygen, Chem. Rev. 103 (2003) 1685-1757.

[10]W.M. Sharman, J.E. van Lier, C.M. Allen, Targeted photodynamic therapy via receptor mediated delivery systems, Adv. Drug Deliv. Rev. 56 (2004) 53-76.

[11]A.S. Derycke, P.A. de Witte, Liposomes for photodynamic therapy, Adv. Drug Deliv. Rev. 56 (2004) 17-30.

[12]T.L. Andresen, S.S. Jensen, K. Jorgensen, Advanced strategies in liposomal cancer therapy: problems and prospects of active and tumor specific drug release, Prog. Lipid Res. 44 (2005) 68-97.

[13]D.K. Chatterjee, L.S. Fong, Y. Zhang, Nanoparticles in photodynamic therapy: an emerging paradigm, Adv. Drug Deliv. Rev. 60 (2008) 1627-1637.

[14]X. Damoiseau, H.J. Schuitmaker, J.W. Lagerberg, M. Hoebeke, Increase of the photosensitizing efficiency of the Bacteriochlorin a by liposome-incorporation, J. Photochem. Photobiol. B. 60 (2001) 50-60.

[15]M.C. Galanou, T.A. Theodossiou, D. Tsiourvas, Z. Sideratou, C.M. Paleos, Interactive transport, subcellular relocation and enhanced phototoxicity of hypericin encapsulated in guanidinylated liposomes via molecular recognition, Photochem. Photobiol. 84 (2008) 1073-1083.

[16]A.A. Gabizon, H. Shmeeda, S. Zalipsky, Pros and cons of the liposome platform in cancer drug targeting, J. Liposome Res. 16 (2006) 175-183.

[17]K. Maruyama, O. Ishida, T. Takizawa, K. Moribe, Possibility of active targeting to tumor tissues with liposomes, Adv. Drug Deliv. Rev. 40 (1999) 89-102.

[18]A. Gijsens, L. Missiaen, W. Merlevede, P. de Witte, Epidermal growth factor-mediated targeting of chlorin e6 selectively potentiates its photodynamic activity, Cancer Res. 60 (2000) 2197-2202.

[19]M. Singh, Transferrin As A targeting ligand for liposomes and anticancer drugs, Curr. Pharm. Des. 5 (1999) 443-451.

[20]P. Sapra, T.M. Allen, Ligand-targeted liposomal anticancer drugs, Prog. Lipid Res. 42 (2003) 439-462.

[21]W. Xia, P.S. Low, Folate-Targeted Therapies for Cancer, J. Med. Chem. (2010) .

[22]N. Parker, M.J. Turk, E. Westrick, J.D. Lewis, P.S. Low, C.P. Leamon, Folate receptor expression in carcinomas and normal tissues determined by a quantitative radioligand binding assay, Anal. Biochem. 338 (2005) 284-293.

[23]R.J. Lee, P.S. Low, Delivery of liposomes into cultured KB cells via folate receptor-mediated endocytosis, J. Biol. Chem. 269 (1994) 3198-3204.

[24]R. Schneider, F. Schmitt, C. Frochot, Y. Fort, N. Lourette, F. Guillemin, J.F. Muller, M. Barberi-Heyob, Design, synthesis, and biological evaluation of folic acid targeted tetraphenylporphyrin as novel photosensitizers for selective photodynamic therapy, Bioorg. Med. Chem. 13 (2005) 2799-2808.

[25]J. Gravier, R. Schneider, C. Frochot, T. Bastogne, F. Schmitt, J. Didelon, F. Guillemin, M. Barberi-Heyob, Improvement of meta-tetra(hydroxyphenyl)chlorin-like photosensitizer selectivity with folate-based targeted delivery. synthesis and in vivo delivery studies, J. Med. Chem. 51 (2008) 3867-3877.

[26]M.M. Qualls, D.H. Thompson, Chloroaluminum phthalocyanine tetrasulfonate delivered via acid-labile diplasmenylcholine-folate liposomes: intracellular localization and synergistic phototoxicity, Int. J. Cancer 93 (2001) 384-392.

[27]R. Hudson, R.W. Boyle, Strategies for selective delivery of photodynamic sensitisers to biological targets, J. Porphyr. Phthalocyanines 8 (2004) 954-975.

[28]D. Bechet, P. Couleaud, C. Frochot, M.L. Viriot, F. Guillemin, M. Barberi-Heyob, Nanoparticles as vehicles for delivery of photodynamic therapy agents, Trends Biotechnol. 26 (2008) 612-621.

[29]K. Stefflova, H. Li, J. Chen, G. Zheng, Peptide-based pharmacomodulation of a cancer-targeted optical imaging and photodynamic therapy agent, Bioconjug. Chem. 18 (2007) 379-388.

[30]B.C. Bae, K. Na, Self-quenching polysaccharide-based nanogels of pullulan/folate-photosensitizer conjugates for photodynamic therapy, Biomaterials 31 (2010) 6325-6335.

[31]F. Postigo, M. Mora, M.A. De Madariaga, S. Nonell, M.L. Sagrista, Incorporation of hydrophobic porphyrins into liposomes: characterization and structural requirements, Int. J. Pharm. 278 (2004) 239-254.

[32]F. Postigo, M.L. Sagrista, M.A. De Madariaga, S. Nonell, M. Mora, Photosensitization of skin fibroblasts and HeLa cells by three chlorin derivatives: Role of chemical structure and delivery vehicle, Biochim. Biophys. Acta 1758 (2006) 583-596.

[33]C.P. Leamon, P.S. Low, Membrane folate-binding proteins are responsible for folate-protein conjugate endocytosis into cultured cells, Biochem. J. 291 (Pt 3) (1993) 855-860.

[34]J.C. Stewart, Colorimetric determination of phospholipids with ammonium ferrothiocyanate, Anal. Biochem. 104 (1980) 10-14.

[35]M.L. Sagrista, F. Postigo, M.A. De Madariaga, R.M. Pinto, S. Caballero, A. Bosch, M.A. Valles, M. Mora, Photodynamic inactivation of viruses by immobilized chlorin-containing liposomes, Journal of Porphyrins and Phthalocyanines 13 (2009) 578-588.

[36]T. Mosmann, Rapid Colorimetric Assay for Cellular Growth and Survival - Application to Proliferation and Cyto-Toxicity Assays, J. Immunol. Methods 65 (1983) 55-63.

[37]P.K. Smith, R.I. Krohn, G.T. Hermanson, A.K. Mallia, F.H. Gartner, M.D. Provenzano, E.K. Fujimoto, N.M. Goeke, B.J. Olson, D.C. Klenk, Measurement of protein using bicinchoninic acid, Anal. Biochem. 150 (1985) 76-85.

[38]H. Hillaireau, P. Couvreur, Nanocarriers' entry into the cell: relevance to drug delivery, Cell Mol. Life Sci. 66 (2009) 2873-2896.

[39]C.P. Leamon, P.S. Low, Delivery of macromolecules into living cells: A method that exploits folate receptor endocytosis, Proc. Natl. Acad. Sci. USA 88 (1991) 5572-5576.

[40]B.A. Kamen, A. Capdevila, Receptor-mediated folate accumulation is regulated by the cellular folate content, Proc. Natl. Acad. Sci. U. S. A. 83 (1986) 5983-5987.

[41]M. Alvarez, A. Villanueva, P. Acedo, M. Canete, J.C. Stockert, Cell death causes relocalization of photosensitizing fluorescent probes, Acta Histochem. (2010) .

[42]J.P. Strachan, S. Gentemann, J. Seth, W.A. Kalsbeck, J.S. Lindsey, D. Holten, D.F. Bocian, Effects of orbital ordering on electronic communication in multiporphyrin arrays, J. Am. Chem. Soc. 119 (1997) 11191-11201.

[43]A. Jimenez-Banzo, X. Ragas, P. Kapusta, S. Nonell, Time-resolved methods in biophysics. 7. Photon counting vs. analog time-resolved singlet oxygen phosphorescence detection, Photochem. Photobiol. Sci. 7 (2008) 1003-1010.

[44]A. Jimenez-Banzo, M.L. Sagrista, M. Mora, S. Nonell, Kinetics of singlet oxygen photosensitization in human skin fibroblasts, Free Radic. Biol. Med. 44 (2008) 1926-1934.

[45]F. Ricchelli, G. Jori, Distribution of porphyrins in the various compartments of unilamellar liposomes of dipalmitoyl-phosphatidylcholine as probed by fluorescence spectroscopy, Photochem. Photobiol. 44 (1986) 151-157.

[46]F. Ciuchi, G. Dinicola, H. Franz, G. Gottarelli, P. Mariani, M.G.P. Bossi, G.P. Spada, Self-Recognition and Self-Assembly of Folic-Acid Salts - Columnar Liquid-Crystalline Polymorphism and the Column Growth-Process, J. Am. Chem. Soc. 116 (1994) 7064-7071.

[47]J.M. Saul, A. Annapragada, J.V. Natarajan, R.V. Bellamkonda, Controlled targeting of liposomal doxorubicin via the folate receptor in vitro, J. Control. Release 92 (2003) 49-67.

[48]J. Wu, Q. Liu, R.J. Lee, A folate receptor-targeted liposomal formulation for paclitaxel, Int. J. Pharm. 316 (2006) 148-153.

[49]N.S. Trivedi, H.W. Wang, A.L. Nieminen, N.L. Oleinick, J.A. Izatt, Quantitative analysis of Pc 4 localization in mouse lymphoma (LY-R) cells via double-label confocal fluorescence microscopy, Photochem. Photobiol. 71 (2000) 634-639.

[50]J.A. Caruso, P.A. Mathieu, J.J. Reiners, Sphingomyelins suppress the targeted disruption of lysosomes/endosomes by the photosensitizer NPe6 during photodynamic therapy, Biochem. J. 392 (2005) 325-334.

[51]T.I. Peng, C.J. Chang, M.J. Guo, Y.H. Wang, J.S. Yu, H.Y. Wu, M.J. Jou, Mitochondrion-targeted photosensitizer enhances the photodynamic effect-induced

mitochondrial dysfunction and apoptosis, Role of the Mitochondria in Human Aging and Disease: From Genes to Cell Signaling 1042 (2005) 419-428.

[52]B.F. P.Tamietti, A.H.A. Machado, M. Maftoum-Costa, N.S. Da Silva, A.C. Tedesco, C. Pacheco-Soares, Analysis of mitochondrial activity related to cell death after PDT with AlPCS4, Photomedicine and Laser Surgery 25 (2007) 175-179.

[53]P.R. Ogilby, C.S. Foote, Chemistry of Singlet Oxygen. 42. Effect of Solvent, Solvent Isotopic Substitution and Temperature on Lifetime of Singlet Molecular Oxygen ($^{1}\text{Ž}_{g}$), J. Am. Chem. Soc. 105 (1983) 3423-3430.

[54]J. Moan, On the diffusion length of singlet oxygen in cells and tissues, J. Photochem. Photobiol. B:Biol. 6 (1990) 343-347.

[55]E. Skovsen, J.W. Snyder, J.D.C. Lambert, P.R. Ogilby, Lifetime and diffusion of singlet oxygen in a cell, J Phys Chem B 109 (2005) 8570-8573.

[56]S. Hackbarth, J. Schlothauer, A. Preuss, B. Roder, New insights to primary photodynamic effects--Singlet oxygen kinetics in living cells, J. Photochem. Photobiol. B. 98 (2010) 173-179.